LEGIBILITY NOTICE

LA-UR -90-2699

SEP 0 7 1990

LA-UR--90-2699

DE90 016568

TITLE HIGH-STRAIN-RATE COMPRESSION AND FRACTURE OF B_4C-ALUMINUM CERMETS

AUTHOR(S) William R. Blumenthal, MST-5

SUBMITTED TO EXPLOMET'90 International Conference on Shock-Wave and High-Strain-Rate Phenomena in Materials, 12-17 August 1990, University of California at San Diego, La Jolla, CA 92093.

Los Alamos National Laboratory
Los Alamos, New Mexico 87545

HIGH-STRAIN-RATE COMPRESSION AND FRACTURE OF B_4C-ALUMINUM CERMETS

W.R. BLUMENTHAL

Materials Science and Technology Division
Los Alamos National Laboratory
Los Alamos, New Mexico 87545, U.S.A.

The compressive behavior of liquid-metal infiltrated boron carbide-aluminum cermets were studied as a function of strain rate, composition, and microstructure. Hopkinson split pressure bar (HSPB) and quasi-static compression tests were conducted using dumb-bell-shaped specimens. Results showed cermet compressive strength to be independent of loading rate. Strength was also found to be independent of the aluminum alloy used to infiltrate pre-sintered 65 vol% B_4C pre-forms. Compositions with the smallest phase size displayed the best strength and ductility.

I. INTRODUCTION

Light-weight cermets (ceramic content > 50 volume %) for armor applications have been of interest for over 20 years [1,2]. These efforts have culminated in the achievement of major breakthroughs in the processing of boron carbide-aluminum and aluminum oxide-aluminum cermets with ceramic contents over 65 vol% within the last five years [3-6]. Characterization of the mechanical response of these cermets is considered to be an important input to their further development and optimization. However, most of the interest in these materials has been devoted to measuring and modelling their fracture toughness and tensile strength [7-9].

Monolithic ceramic tensile failure is typically preceded by extremely localized permanent deformation associated with the initiation and/or propagation of a small number of flaws. Hence, tensile failure will be dependent on the rate of loading only when it is high enough to influence the dominant crack initiation and/or crack propagation mechanism [10]. This is in contrast to the origins of rate dependence in ductile metals which are related to microstructure evolution and the kinetics of deformation mechanisms. Cermets can exhibit measurable permanent deformation prior to failure in both tension and compression which may be associated with microcrack (damage) accumulation. Hence cermet compressive strength may exhibit novel strain rate dependence.

The primary focus of this work was to determine the influence of processing variables (i.e. microstructure and composition) on the compressive behavior of liquid metal infiltrated boron carbide aluminum cermets as a function of strain rate.

Recently there have been renewed attempts to correlate the compressive behavior of monolithic ceramics with their ballistic performance [11]. These studies emphasize the necessity for reliable materials property measurements obtained usi... ... n and ballistic test methods. Quasi-static compressio... ... materials have continued to evolve up to the preser... [12,13]. It has been recognized in these studies that tensile stresses can readily develop at specimen interfaces for a variety of reasons and can therefore control the measured failure strength. A proven method for minimizing these interface effects is to use a reduced-gage-section (dumbbell-shaped) specimen [14,15]. The present study extends the use of the dumbbell-shaped specimen to the high strain rate regime.

II. MATERIALS

Four series of cermets were fabricated at the University of Washington by infiltrating liquid aluminum into partially sintered boron carbide pre-forms [4]. Fabrication variables included: phase volume fraction, phase size, and metal phase composition. B_4C volume fractions of 65% and 80% were studied and represent practical boundaries for strong, yet open porosity pre-forms. Average phase sizes of 2.4 and 6.3 microns were measured for the Al and B_4C, respectively, in a "fine-grained" 65 vol% B_4C-pure Al series. A "coarse-grained" version contains average phase sizes of 21 and 47 microns for the Al and B_4C, respectively. Finally, two series of cermets were made by infiltrating either pure aluminum or 7075 aluminum alloy into 65 vol% B_4C pre-forms. All cermets tested were nominally fully dense (less than 2% porosity).

III. EXPERIMENTAL PROCEDURES

A. *SPECIMEN GEOMETRY*

All tests were conducted using a scaled-down version of the dumbbell-shaped specimen designed by Tracy [14]. Specimens have over-all dimensions of 13 mm x 4.4 mm with nominal gage length of 5 mm and gage diameter of 2.2 mm. The length of this specimen is comparable to the length of right-circular-cylinder specimen (12.5 mm x 6.25 mm) used by Lankford for HSPB studies of aluminum oxide [16]. This specimen length is short enough to permit equilibration of the stresses within the sample prior to failure at strain rates of 10^3 s^{-1} for these high sound speed materials ($C_1 > 9 \times 10^3$ m/s).

Specimen strain is determined in situ using three independent strain gages attached at uniform intervals about the specimen gage circumference. This configuration allows the bending stresses to be determined. Specimen strain gages are required because the "effective" gage length is not known precisely, especially after the gage section yields (permanently deforms).

B. *HOPKINSON BAR COMPRESSION*

Hopkinson split pressure bar tests were conducted using 12.5 mm diameter, 350 ksi yield strength, maraging steel bars at a nominal strain rate of 10^3 s^{-1}. Specimen stress was calculated from the transmitted bar in the conventional manner as the product of the bar stress and the ratio of bar-to-specimen cross-sectional areas. High band-width (> 3 MHz) strain gage amplifiers and digitizing oscilloscopes were used with a sampling rate of 10^7 points/sec.

Two types of experiments were conducted dynamically: 1) fracture strength and 2) recovery tests. Recovery tests were used to determined yield points and fracture strengths more precisely.

C. QUASI-STATIC COMPRESSION

Quasi-static compression tests were conducted using an Instron Model 1125 testing machine fitted with a precision-machined sub-press. Specimens were aligned in a precision V-block with tungsten carbide loading rams at each end. Testing was performed at a nominal strain rate of 10^{-4} s^{-1}. Specimen strain was obtained in the same manner as with the HSPB, but at a sampling rate of 10 points/sec. and with direct synchronization of the load record.

D. DATA REDUCTION

Quasi-static compression tests were analyzed by calculating the average specimen strain and the bending stress resulting from load eccentricity. The bending stresses were between 5% to 20% of the compressive stress.

In order to analyze the HSPB tests, the bar and specimen records must be synchronized. Recovery tests were used to determine the proper time adjustment between the records to within a few tenths of a microsecond.

IV. RESULTS

Fig. 1 shows a summary of stress versus average strain for the four cermets as a function of strain rate. A comparison of quasi-static and Hopkinson bar results shows that up to strain rates of 10^3 s^{-1}, the peak strength of all the cermets is independent of loading rate. Compression strength is also shown to be independent of the aluminum alloy infiltrate for the fine grained 65 vol% B_4C composition. The fine-grained 65% and 80% B_4C compositions (average aluminum phase size = 2.5 microns) all yield at about 1.3% strain. However, the coarse-grained 65 vol% B_4C composition (average aluminum phase size = 21 microns) yields at about 0.9% strain. Also stresses measured quasi-statically did not exhibit a decay after peaking and the maximum strains were generally much less than those measured dynamically. This illustrates one advantage of the HSPB technique; namely, the sampling rate allows more resolution of the failure event.

The 80 vol% B_4C cermet exhibits twice the ultimate strength compared to the fine grained 65 vol% B_4C cermets primarily due to its higher elastic modulus. Mechanical moduli (stress/total strain) at an arbitrary strain of 1% is plotted along with the ultrasonic values (zero strain) and the predictions from laminate composite theories (Voigt and Reuss) in Fig. 2. Isotropic composites generally behave as the average of Reuss and Voigt solids as exhibited by the ultrasonic values. However, under compressive strain, the modulus is observed to decay towards the value of a Reuss solid. In the case of the 65 vol% B_4C cermets the decay is complete to the Reuss value (a bounding condition). Recovery tests show that this behavior is reversible. A simple analysis (Poisson's ratio and stress concentration effects are neglected) of the individual phase strains is demonstrated in Fig. 3 by assuming the 65 vol% B_4C-Al cermets behave as Reuss solids and the 80 vol% B_4C-Al cermet behaves as a Reuss-Voigt-average solid. This analysis indicates that the average elastic strain supported by the aluminum phase is quite high (> 3%) for the 2.5 micron Al phase size cermets prior to the composite yielding. However, the coarse-grained 65 vol% B_4C-Al cermet (21 micron Al phase size) only supports 2% strain in the aluminum phase. The reasons for this phase size effect on the strength are not clear. Fig. 4, a plot of log strength versus log phase size, indicates that neither phase exhibits Hall-Petch behavior. Undoubtedly the aluminum phase is being constrained by the rigid B_4C structure which significantly increases its flow strength as observed in tension loading [17]. Perhaps this constraint is sensitive to the Al phase size or strength of the B_4C.

Fractography of failed specimens show fracture angles of between 25 to 40 degrees from the compression axis (35 degrees is typical). A previous investigation [18] discovered networks of microcracks intersecting the fracture surface of the fine-grained compositions implying that the yield behavior is related to damage accumulation. Sliding damage on several planes also suggested multiple sources of failure initiation. However, failure of the lower strength, coarse-grained cermet did not show sliding striations or coalesced microcracks implying little damage accumulation or aluminum flow occurs during failure.

V. CONCLUSIONS

The HSPB technique possesses distinct advantages: 1) high time resolution (0.1 microsecond) permits details of the failure to be observed. 2) eccentricity (misalignment) appears to be somewhat lower due to the high rate of load application. 3) The amplitude and duration of applied load can be precisely controlled allowing for iterative (recovery) testing.

The compressive behavior of liquid-metal infiltrated boron carbide-aluminum cermets were studied as a function of strain rate, composition, and microstructure. Results showed cermet compressive strength to be independent of loading rate. Strength was also found to be independent of the aluminum alloy used to infiltrate pre-sintered 65 vol% B_4C pre-forms. Compositions with the smallest phase size (both B_4C and Al) displayed the highest strength and ductility.

REFERENCES

1 M.L. Wilkins, C.F. Cline, and C.A. Honodel, *Light Armor*, UCRL-71817,

Lawrence Livermore National Laboratory, Livermore, CA, 1969.

2. M.W. Lindley and G.E. Gazza, *Some New Potential Ceramic-Metal Armor Materials Fabricated by Liquid Metal Infiltration*, AMMRC-TR-73-39, AD-769742, U.S. Army Materials Technology Laboratory, Watertown, MA, 1973.

3. D.C. Halverson, A.J. Pyzik, and I.A. Aksay, *Ceram. Engin. and Sci. Proc.*, 6: 736 (1985).

4. A.J. Pyzik, and I.A. Aksay, *U.S. Patent 4,702,770* (1987).

5. D.C. Halverson and R.L. Landingham, *U.S. Patent 4,718,941* (1988).

6. M.S. Newkirk, A.W. Urquhart, H.R. Zwicker, and E. Brevel, *J. Mater. Res.*, *1:* 81 (1986).

7. L.S. Sigl, P.A. Mataga, B.J. Dalgleish, R.M. Meeking, and A.G. Evans, Acta Metall., *36:* 945 (1988).

8. B.D. Flinn, M. Ruhle, and A.G. Evans, Acta Metall., *37:* 3001 (1989).

9. M.K. Aghajanian, N.H. Macmillan, C.R. Kennedy, S.J. Luszcz, and R. Roy, J. Mat. Sci., *24:* 658 (1989).

10. M.E. Kipp, D.E. Grady, and E.P. Chen, Int. Journ. of Fracture, *16: 471* (1980).

11. Z. Rosenberg and Y Yeshurun, Int. Journ. of Impact Engng., *7: 357* (1988).

12. S.A. Bortz, and T.B. Wade in *Structural Ceramics and Testing of Brittle Materials*, S.J. Acquaviva and S.A. Bortz (eds.), Gordon and Breach Science, New York, 1968, Chap. III, p. 47.

13. G. Sines and M. Adams in *Fracture Mechanics of Ceramics*, Vol. 3, R.C. Bradt, D.P.H. Hasselman and F.F. Lange (eds.), Plenum Press, New York, 1977, p. 403.

14. C.A. Tracy, Jrnl. of Testing and Evaluation, *15: 14* (1987).

15. W.F. Brace in *State of Stress in the Earth's Crust*, W.R.Judd (ed.), American Elsevier, New York, 1964, p. 110.

16. J. Lankford, Jrnl. of Material Science, *12: 791* (1977).

17. M.F. Ashby, F.J. Blunt, and M. Bannister, Acta Metall., *37:* 1847 (1989).

18. W.R. Blumenthal and G.T. Gray III, in *Mechanical Properties of Materials at High Rates of Strain 1989*, J. Harding (ed.), Inst. of Phys. Conf. Series #102, J.W. Arrowsmith Ltd., Bristol, England, 1989, p. 363.

FIG. 1 *Compression stress-strain curves.*

FIG. 2 *Experimental and laminate theory predictions of cermet modulus as a function of composition.*

FIG. 3 *Aluminum phase strain analysis assuming laminate theory versus cermet strain.*

FIG. 4 *Power-law dependence of the compressive strength on constituent phase size.*

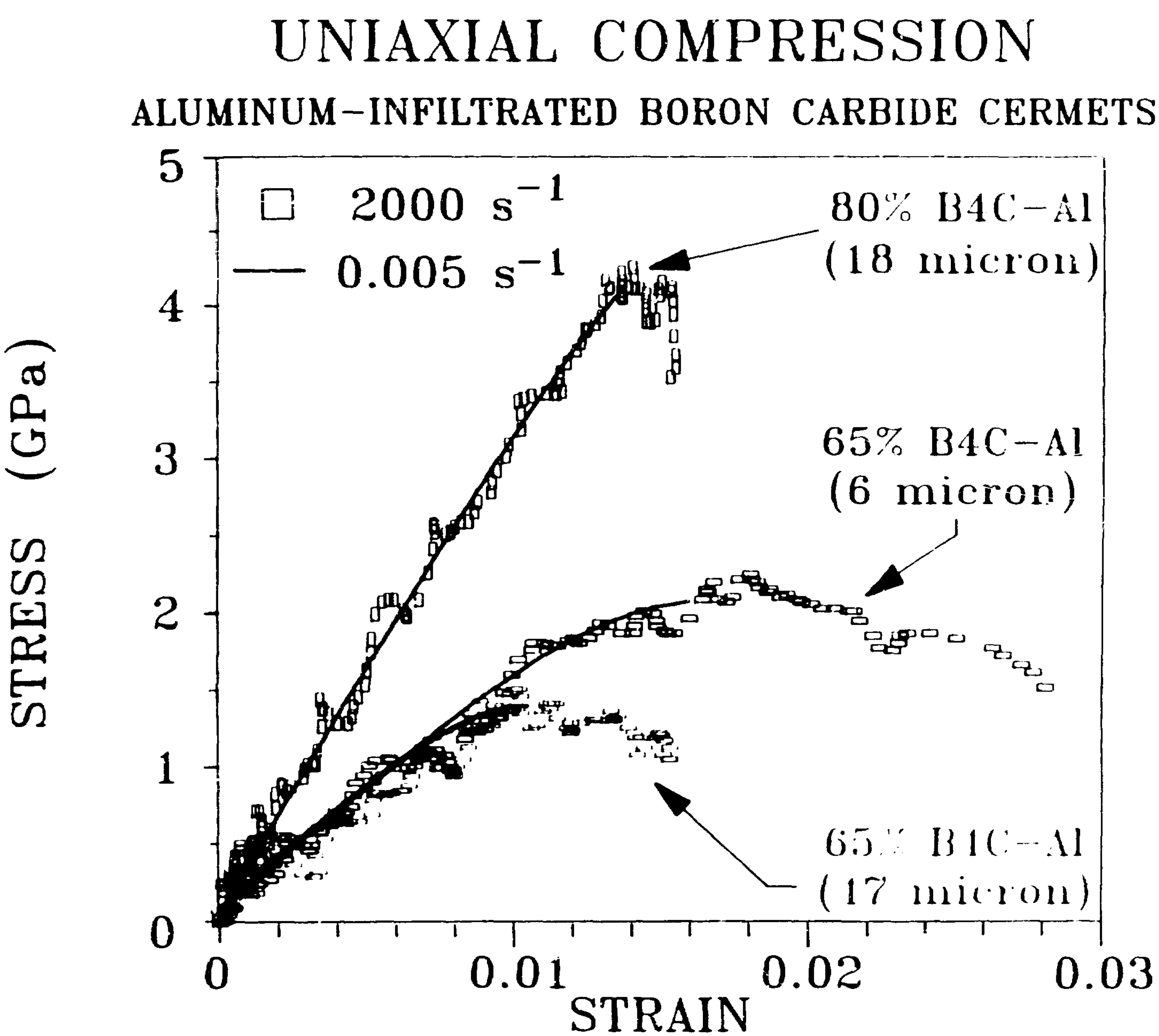
UNIAXIAL COMPRESSION
ALUMINUM-INFILTRATED BORON CARBIDE CERMETS
2000 s^-1
0.005 s^-1
80% B4C-Al
(18 micron)
65% B4C-Al
(6 micron)
65% B4C-Al
(17 micron)
STRESS (GPa)
STRAIN
0
1
2
3
4
5
0
0.01
0.02
0.03

FIGURE 1

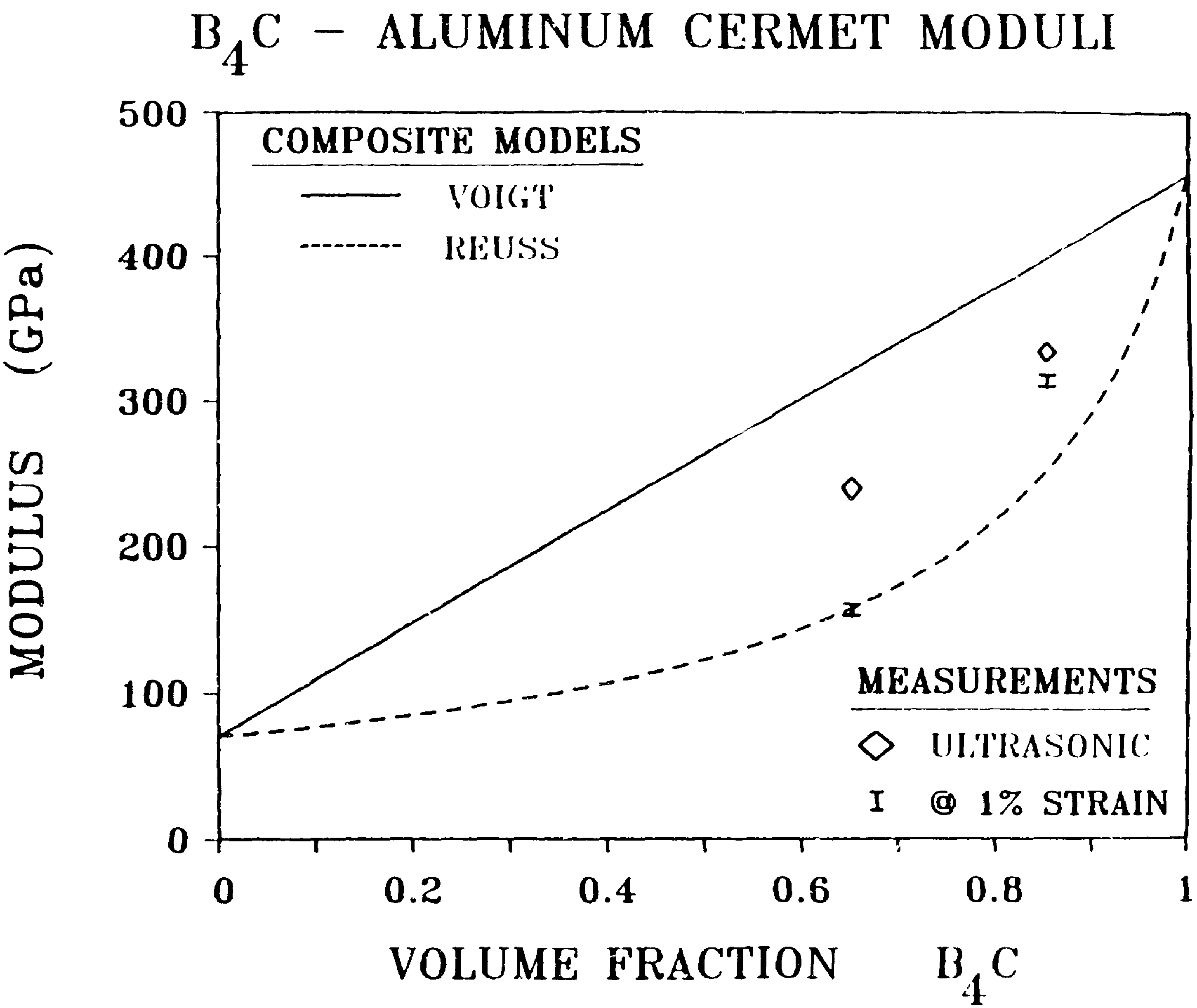
B4C – ALUMINUM CERMET MODULI
MODULUS (GPa)
VOLUME FRACTION B4C
COMPOSITE MODELS
VOIGT
REUSS
MEASUREMENTS
ULTRASONIC
@ 1% STRAIN
0
100
200
300
400
500
0
0.2
0.4
0.6
0.8
1

FIGURE 2

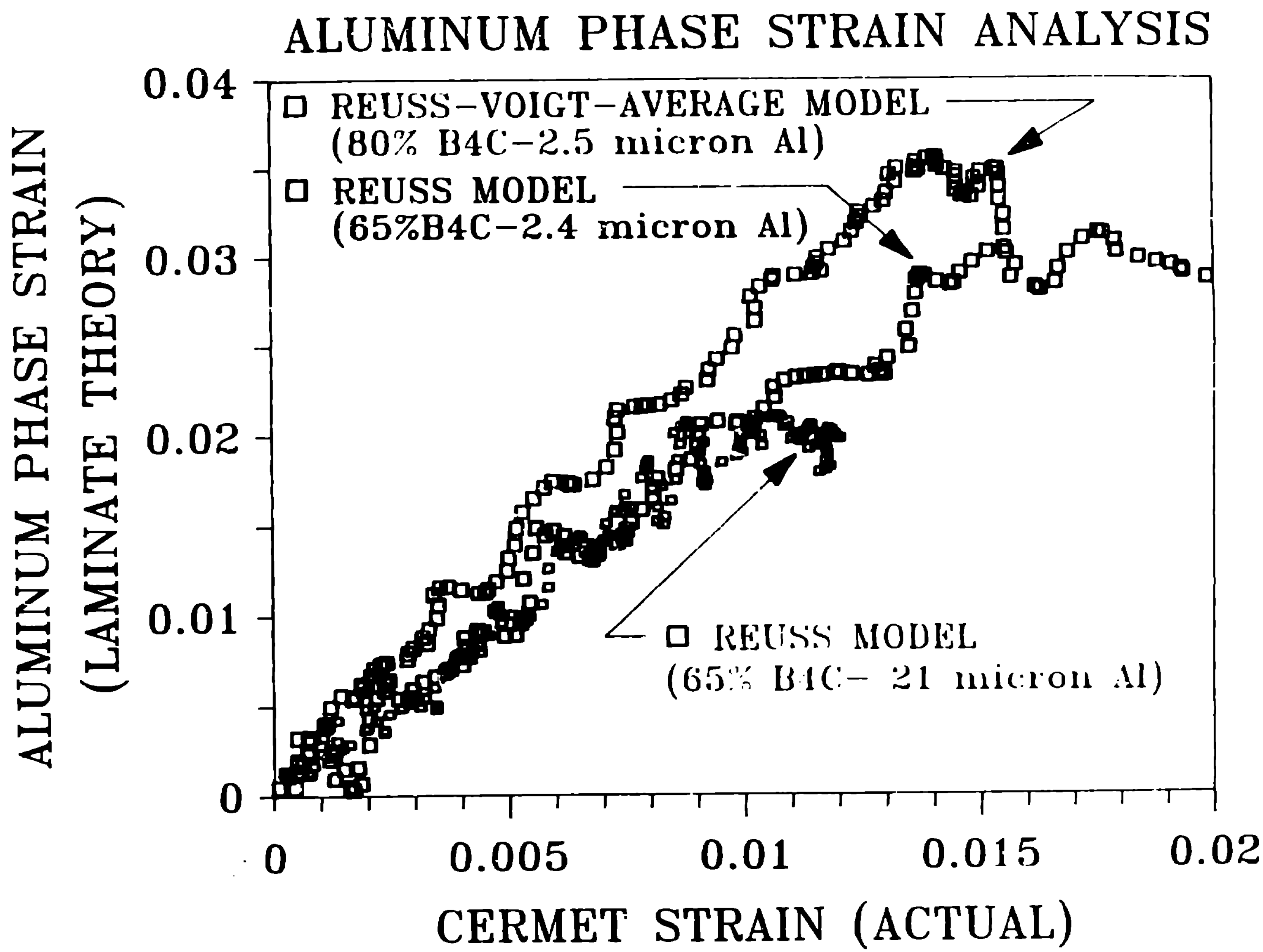
ALUMINUM PHASE STRAIN ANALYSIS
REUSS-VOIGT-AVERAGE MODEL
(80% B4C-2.5 micron Al)
REUSS MODEL
(65%B4C-2.4 micron Al)
REUSS MODEL
(65% B4C- 21 micron Al)
ALUMINUM PHASE STRAIN
(LAMINATE THEORY)
0.04
0.03
0.02
0.01
0
0
0.005
0.01
0.015
0.02
CERMET STRAIN (ACTUAL)

FIGURE 3

COMPRESSIVE STRENGTH vs PHASE SIZE

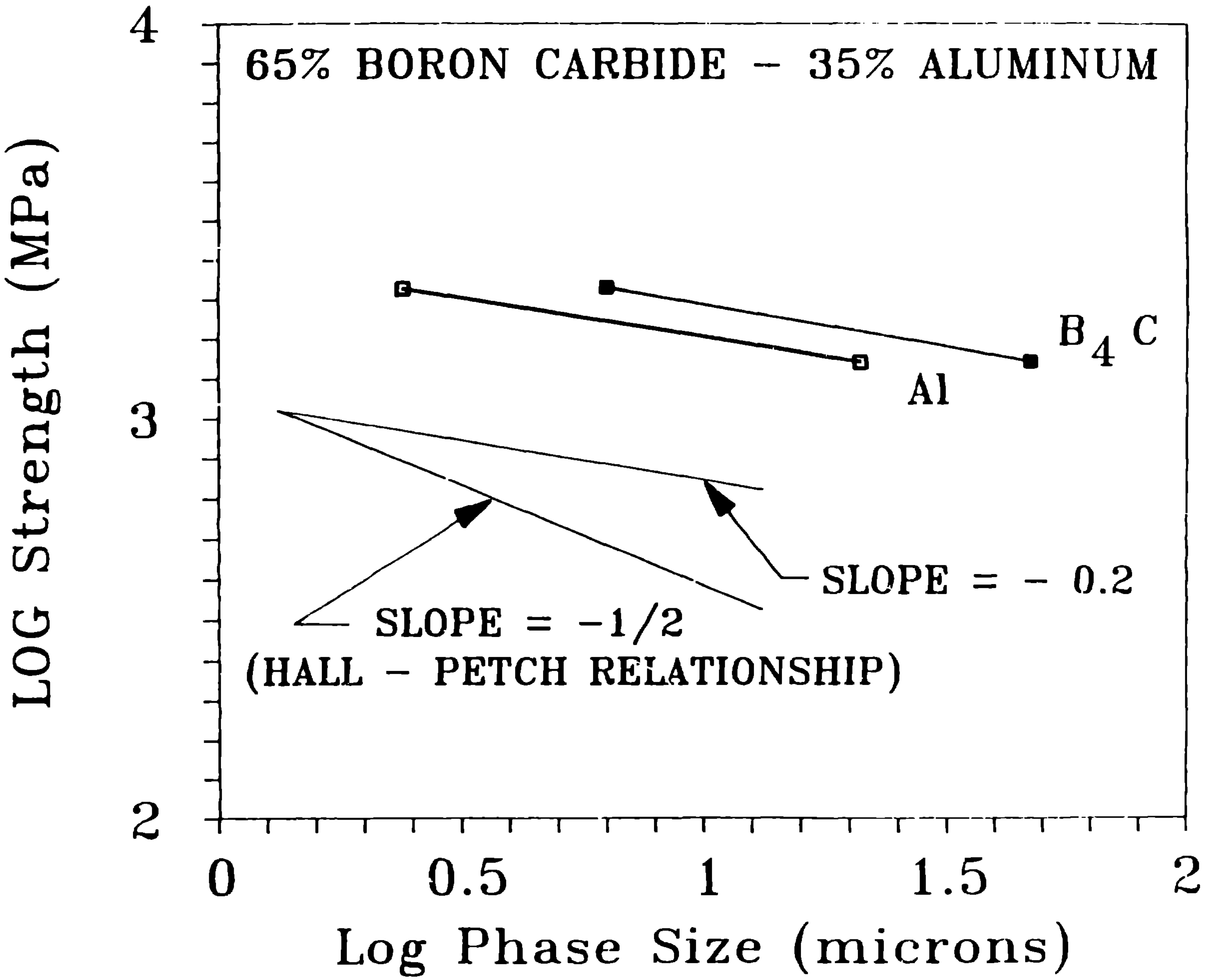

FIGURE 4